

# Edge-Enhanced Dilated Residual Attention Network for Multimodal Medical Image Fusion

*IEEE BIBM 2024 Short Paper*

**Meng (Simon) Zhou**<sup>\*1</sup>, Yuxuan Zhang<sup>\*1</sup>, Xiaolan Xu<sup>1</sup>, Jiayi Wang<sup>2</sup>, and  
Farzad Khalvati<sup>1,3</sup>

<sup>1</sup> Department of Computer Science, University of Toronto

<sup>2</sup> Desautels Faculty of Management, McGill University

<sup>3</sup> Department of Medical Imaging, University of Toronto



UNIVERSITY OF  
TORONTO



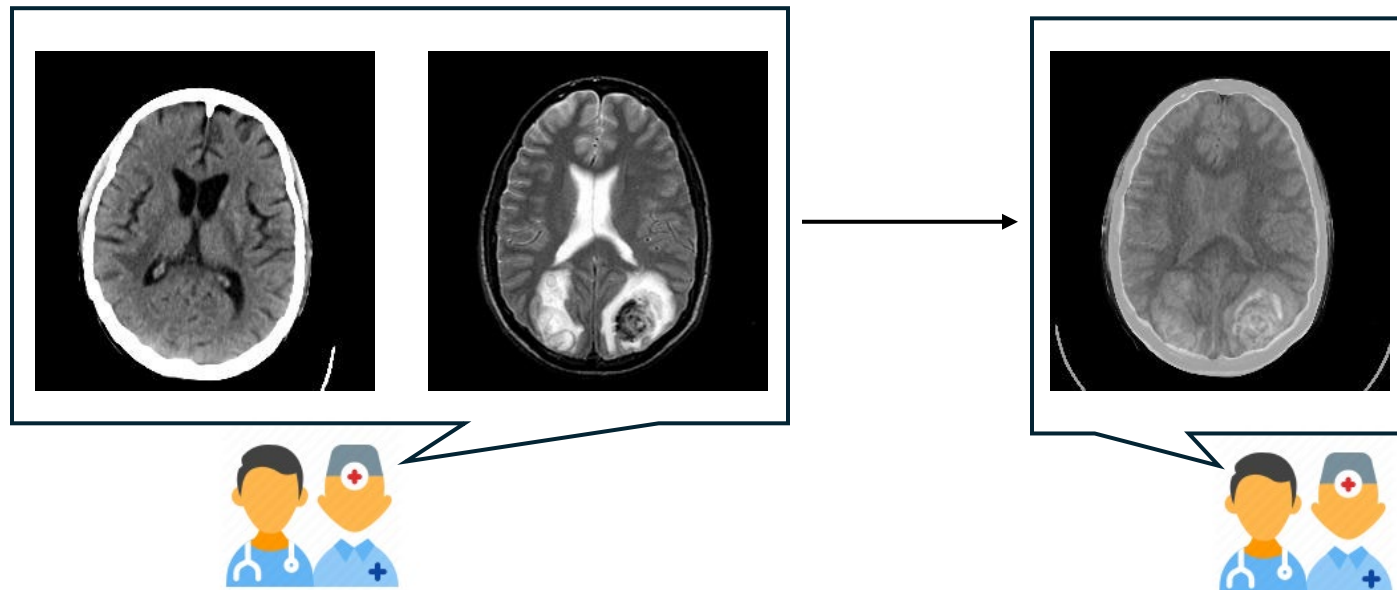
McGill  
UNIVERSITY

# Outline

- Background
- Related Works
- Problem
- Proposed Method
- Experiments
- Conclusions and Future work

# Background

- Multimodal image fusion plays an increasingly prominent role in clinical diagnosis.
- It aims to aggregate common and complementary information from different image modalities as well as integrate the information to generate more clearer and informative images
- Physicians must analyze multiple images to make informed decisions, a process that is both time-consuming and laborious.



# Related works

- CNN-based:
  - IFCNN [1]: CNN-based image fusion framework for multi-focus, infrared-visible, and multimodal medical image fusion. Elementwise fusion rules to combine feature maps directly.
  - MSRPAN [2]: Residual pyramid attention network for multimodal medical image fusion and Feature Energy Ratio Strategy to fuse feature maps
  - MSDRA [3]: Double residual attention network for multimodal medical image fusion and uses weighted L1 Norm to fuse feature maps



## *Limitations...*

1. Losing the structural information and edge details, which are crucial for medical images
2. Lack of multiscale learning capabilities

[1] Zhang, Y., Liu, Y., Sun, P., Yan, H., Zhao, X., & Zhang, L. (2020). IFCNN: A general image fusion framework based on convolutional neural network. *Information Fusion*, 54, 99-118.  
[2] Fu, J., Li, W., Du, J., & Huang, Y. (2021). A multiscale residual pyramid attention network for medical image fusion. *Biomedical Signal Processing and Control*, 66, 102488.  
[3] Li, W., Peng, X., Fu, J., Wang, G., Huang, Y., & Chao, F. (2022). A multiscale double-branch residual attention network for anatomical–functional medical image fusion. *Computers in biology and medicine*, 141, 105005.

# Related works

- Transformer-based:
  - SwinFusion [3]: Combining a CNN feature extractor with a cross-domain transformer model to fuse local and global information.
  - MRSCFusion [4]: Combining a multiscale CNN model and applied residual Swin Transformer layers to fuse cross-domain information.
  - MACTFusion [5]: Light-weight cross modality transformer with window and grid attention.



## *Limitations...*

1. Computational cost is high and hinders the clinical application.
2. Applying the fusion method to real clinical diagnosis tasks is not fully explored.

[3] Ma, J., Tang, L., Fan, F., Huang, J., Mei, X., & Ma, Y. (2022). SwinFusion: Cross-domain long-range learning for general image fusion via swin transformer. *IEEE/CAA Journal of Automatica Sinica*, 9(7), 1200-1217.

[4] Xie, X., Zhang, X., Ye, S., Xiong, D., Ouyang, L., Yang, B., ... & Wan, Y. (2023). MRSCFusion: Joint residual Swin transformer and multiscale CNN for unsupervised multimodal medical image fusion. *IEEE Transactions on Instrumentation and Measurement*.

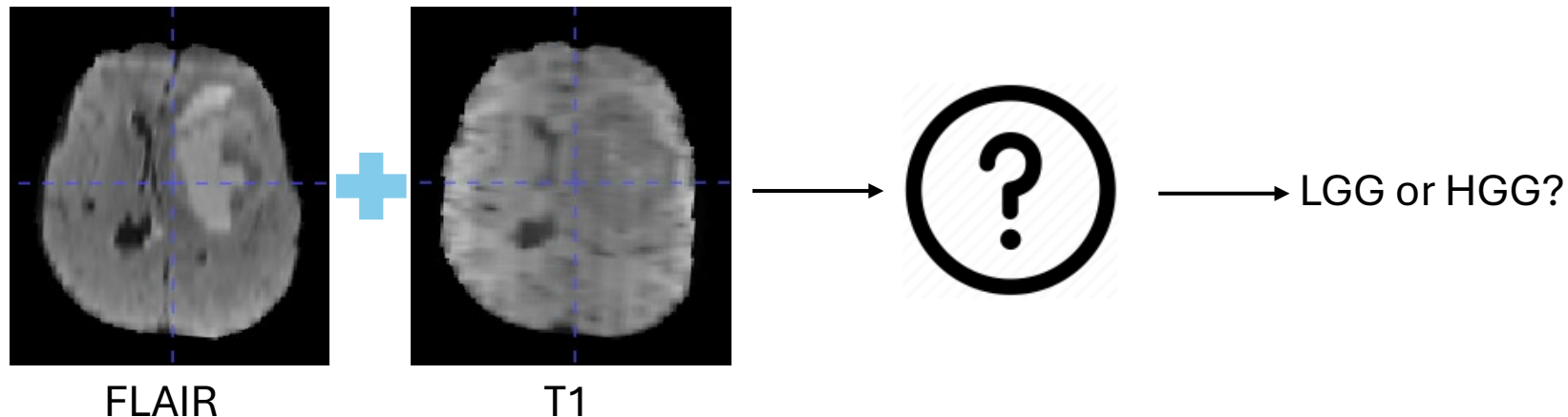
[5] Xie, X., Zhang, X., Tang, X., Zhao, J., Xiong, D., Ouyang, L., ... & Teo, K. L. (2024). MACTFusion: Lightweight Cross Transformer for Adaptive Multimodal Medical Image Fusion. *IEEE Journal of Biomedical and Health Informatics*.

# Problem

- Two most common fusion tasks in medical imaging: MRI-CT and MRI-SPECT fusion tasks

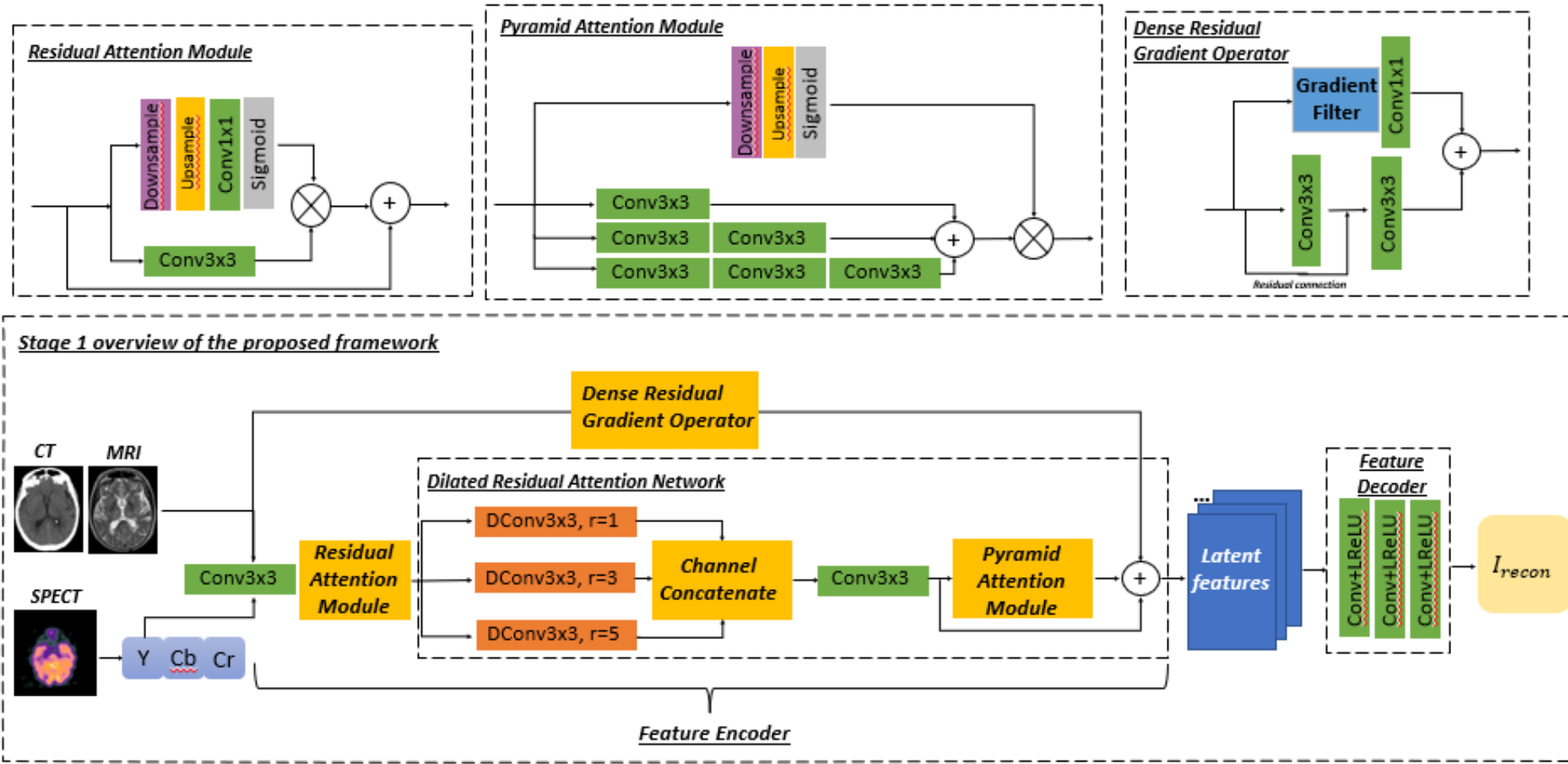


- To further evaluate the effectiveness of the fusion method, we apply it to a downstream clinical brain tumor pathology classification task between Low-Grade and High-Grade Gliomas.



# Proposed Method

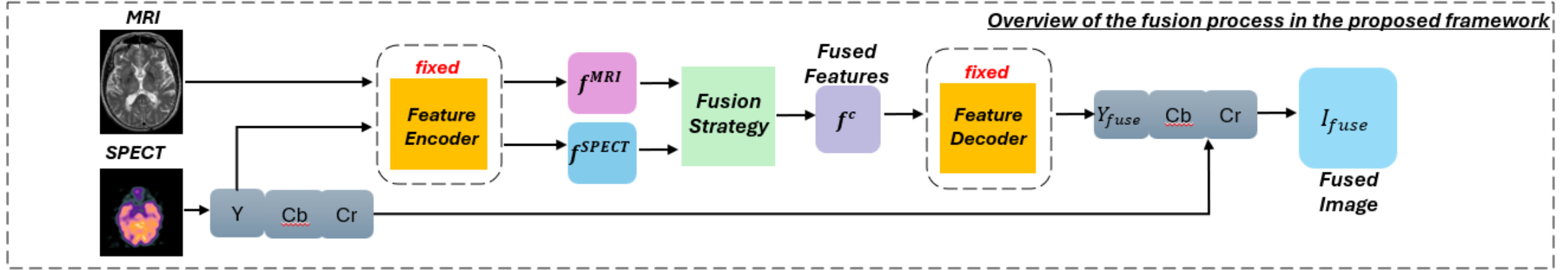
## Stage 1



Asymmetric Autoencoder (Stage 1 model) in the proposed framework

# Proposed Method

## Stage 2



## SFNN Strategy

$$W_k = \frac{\phi(\|S(x_i)^k\|_*)}{\sum_{k=1}^C \phi(\|S(x_i)^k\|_*)}$$

## Loss function

$$\mathcal{L}_{pixel} = \|x - \hat{x}\|_2^2, \quad \mathcal{L}_{grad} = \|\nabla x - \nabla \hat{x}\|_2^2,$$

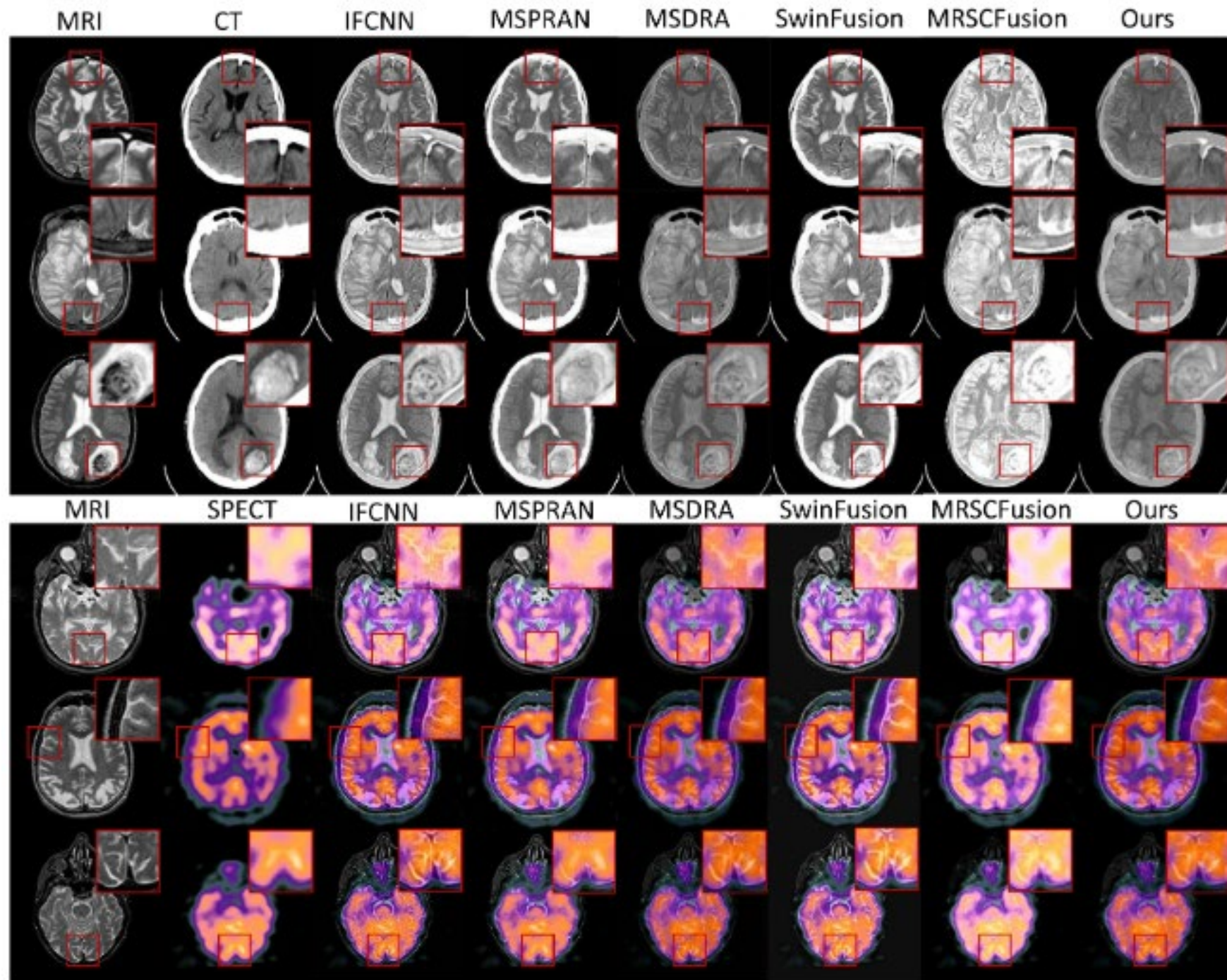
$$\mathcal{L}_{perp} = \sum_{k=1}^C \|f_i^k(x) - f_i^k(\hat{x})\|_2^2$$

$$\mathcal{L}(\theta) = \mathcal{L}_{pixel} + \lambda_1 * \mathcal{L}_{grad} + \lambda_2 * \mathcal{L}_{perp}$$



# Experiments

- Qualitative Results



# Experiments

- Quantitative Results

Dataset	Method	PSNR	SSIM	FMI	FSIM	EN
MRI-CT	IFCNN [7]	<u>15.594±0.112</u>	0.700±0.015	0.870±0.012	0.801±0.001	8.968±0.227
	MSRPAN [8]	14.790±0.233	0.749±0.003	0.744±0.001	0.804±0.001	7.773±0.273
	MSDRA [9]	15.308±0.437	0.742±0.037	0.872±0.002	0.788±0.005	<u>9.554±0.767</u>
	SwinFusion [13]	14.962±0.173	<b>0.768±0.007</b>	<u>0.882±0.002</u>	<u>0.810±0.001</u>	8.445±0.078
	MRSCFusion [1]	14.476±0.205	0.713±0.012	<u>0.877±0.006</u>	<u>0.791±0.010</u>	7.544±0.232
	EH-DRAN(Ours)	<b>16.830±0.490</b>	<u>0.753±0.007</u>	<b>0.883±0.005</b>	<b>0.820±0.003</b>	<b>10.727±0.531</b>
MRI-SPECT	IFCNN [7]	<u>19.728±0.228</u>	0.721±0.025	<u>0.846±0.062</u>	0.783±0.027	10.167±0.429
	MSRPAN [8]	<u>19.174±0.046</u>	0.732±0.002	<u>0.838±0.003</u>	0.793±0.002	9.737±0.202
	MSDRA [9]	19.662±0.165	0.725±0.003	0.839±0.003	0.794±0.003	10.784±0.447
	SwinFusion [13]	17.557±0.021	0.728±0.004	0.808±0.007	<u>0.819±0.011</u>	<b>13.066±0.428</b>
	MRSCFusion [1]	18.412±0.211	<u>0.734±0.012</u>	0.827±0.009	0.814±0.006	9.87±0.600
	EH-DRAN(Ours)	<b>21.455±0.071</b>	<b>0.736±0.002</b>	<b>0.876±0.004</b>	<b>0.843±0.003</b>	11.970±0.538

**Bold** and underline numbers represent the best and second-best results for each dataset, respectively

# Experiments

- Ablation study

Dataset	Method	PSNR	SSIM	FMI	FSIM	Entropy
MRI-CT	Base Model	15.623±0.032	0.745±0.013	0.878±0.003	0.802±0.003	9.122±0.706
	Base Model+ $\mathcal{L}_{grad}$	16.355±0.038	0.749±0.010	0.881±0.002	0.818±0.002	9.771±0.528
	Base Model+ $\mathcal{L}_{grad}$ +DRGO	<b>16.830±0.490</b>	<b>0.753±0.007</b>	<b>0.883±0.005</b>	<b>0.820±0.003</b>	<b>10.727±0.531</b>
MRI-SPECT	Base Model	20.698±0.002	<b>0.743±0.008</b>	0.833±0.006	0.836±0.005	10.010±0.563
	Base Model+ $\mathcal{L}_{grad}$	20.738±0.026	0.740±0.011	0.837±0.002	0.838±0.004	10.454±0.426
	Base Model+ $\mathcal{L}_{grad}$ +DRGO	<b>21.455±0.071</b>	0.736±0.002	<b>0.876±0.004</b>	<b>0.843±0.003</b>	<b>11.970±0.538</b>

- Fusion time comparison

	IFCNN	MSRPAN	MSDRA	SwinFusion	MRSCFusion	Ours
Params(M)	0.08	0.10	0.20	0.97	23.00	0.50
Time(s)	0.89	0.79	0.81	1.31	2.85	1.26

# Experiments

- Results on ROI-based LGG/HGG tumor pathology types classification

---

	AUC	F1-Score	Accuracy
T2 (1-channel)	0.722±0.021	0.703±0.018	0.604±0.037
FLAIR (1-channel)	0.727±0.024	0.701±0.008	0.611±0.017
T2+FLAIR (2-channel)	0.723±0.028	0.717±0.012	0.640±0.015
Fused (1-channel)	<b>0.769±0.003</b>	<b>0.723±0.006</b>	<b>0.640±0.011</b>

---

# Conclusions and Future Work

- Novel asymmetric autoencoder architecture incorporating a Dilated Residual Attention Network (DRAN) for effective multi-scale feature extraction
- Integrated a Dense Residual Gradient Operator (DRGO) as an edge enhancer to capture fine-grained edge details
- Introduced a family of parameter-free fusion strategies for multimodal image fusion, designed to operate without requiring parameter computation during both training and inference phases
- Extensive evaluated on three datasets to valid the effectiveness of the proposed approach
- **Future Work: Extend to 3D, Explore Mamba-based methods.**

# Thank you for your listening

- Code:



- Arxiv extended version:

